Three-Dimensional Shallow Water Acoustics

Dr. Ying-Tsong Lin
Applied Ocean Physics and Engineering Department
Woods Hole Oceanographic Institution
Woods Hole, MA 02543
phone: (508) 289-2329 fax: (508) 457-2194 email: ytlin@whoi.edu

Award Number: N00014-13-1-0026

LONG-TERM GOALS

Both physical oceanographic processes and marine geological features in the continental shelf can cause the medium properties to have lateral heterogeneity, so horizontal refraction of sound can occur and produce significant three-dimensional (3-D) sound propagation effects. The long-term goals of this project are targeted on understanding the 3-D acoustic effects caused by the environmental factors existing commonly in the continental shelf and shelfbreak areas.

OBJECTIVES

One of the research objectives of this project is to develop efficient and accurate 3D models (both theoretical and numerical models) for studying underwater sound propagation in 3-D ocean environments. The ultimate scientific objective of the proposed work is to study the underlying physics of the 3-D sound propagation effects caused jointly by physical oceanographic processes and geological features. To achieve this goal, individual environmental factor will be first studied and then considered jointly with a unified ocean, seabed and acoustic model. Another major objective is to develop a tangent linear model to predict acoustic fluctuations due to 3-D sound speed perturbation in the water column. This model will be useful for the sensitivity analysis to assess the joint ocean and seabed effects.

APPROACH

The technical approaches employed in the 3D sound propagation study include theoretical analysis, numerical computation and real data analysis. A 3-D normal mode method has been used to study canonical environmental models of shelfbreak front systems [1] and nonlinear internal wave ducts [2-3]. 3-D parabolic-equation (PE) wave propagation models with improved split-step marching algorithms [4-6] are used to study sound propagation in realistic environments. When the acoustic mode coupling can be neglected, a vertical-mode horizontal-PE model is used. These PE models employ the following higher order operator splitting to increase the PE approximation accuracy.

$$\sqrt{1+\mathcal{A}+\mathcal{B}} \cong \sqrt{1+\mathcal{A}} + \left(-1+\sqrt{1+\mathcal{B}}\right) - \frac{1}{2}\left(-1+\sqrt{1+\mathcal{A}}\right)\left(-1+\sqrt{1+\mathcal{B}}\right) - \frac{1}{2}\left(-1+\sqrt{1+\mathcal{B}}\right)\left(-1+\sqrt{1+\mathcal{A}}\right), \tag{1}$$

Report Documentation Page

Form Approved
OMB No. 0704-0188

1. REPORT DATE	2. REPORT TYPE	3. DATES COVERED
30 SEP 2013		**00-00-2013 to 00-00-2013**

4. TITLE AND SUBTITLE	5a. CONTRACT NUMBER
Three-Dimensional Shallow Water Acoustics	5b. GRANT NUMBER
	5c. PROGRAM ELEMENT NUMBER
6. AUTHOR(S)	5d. PROJECT NUMBER
	5e. TASK NUMBER
	5f. WORK UNIT NUMBER
7. PERFORMING ORGANIZATION NAME(S) AND ADDRESS(ES) **Woods Hole Oceanographic Institution,Applied Ocean Physics and Engineering Department,Woods Hole,MA,02543**	8. PERFORMING ORGANIZATION REPORT NUMBER
9. SPONSORING/MONITORING AGENCY NAME(S) AND ADDRESS(ES)	10. SPONSOR/MONITOR'S ACRONYM(S)
	11. SPONSOR/MONITOR'S REPORT NUMBER(S)

12. DISTRIBUTION/AVAILABILITY STATEMENT
Approved for public release; distribution unlimited

13. SUPPLEMENTARY NOTES

14. ABSTRACT

15. SUBJECT TERMS

16. SECURITY CLASSIFICATION OF:			17. LIMITATION OF ABSTRACT	18. NUMBER OF PAGES	19a. NAME OF RESPONSIBLE PERSON
a. REPORT	b. ABSTRACT	c. THIS PAGE			
unclassified	**unclassified**	**unclassified**	**Same as Report (SAR)**	**12**	

where $\mathcal{A}$ and $\mathcal{B}$ are two different operators. In the split-step Fourier PE, they are the free-space propagator and the medium phase speed anomalies, respectively [5]. In the split-step Padé PE, they are the derivations in the horizontal and vertical directions [6].

Another numerical method to be used is a tangent linear model to predict acoustic fluctuations due to 3-D sound speed perturbation in the water column. This model has been developed and published [7] this year, and it will be briefed in the next section.

During the Quantifying, Predicting, and Exploiting (QPE) Uncertainty Experiment in 2009 [8-9], mobile acoustic sources were deployed to study underwater sound propagation in the area of North Mein-Hua Canyon northeast of Taiwan. With the hydrophone data received on bottom mounted vertical arrays, we can obtain transmission loss (TL) measurements [10], as well as probability of dectection, which will be briefed in the next section.

WORK COMPLETED

The tasks completed in the year are described below.

1. 3-D higher-order tangent linear PE model

The PE approximation is an effective numerical technique for modeling underwater sound propagation in the ocean. This technique transforms the Helmholtz wave equation into a one-way wave equation that can be solved by a variety of marching algorithms. A higher order tangent linear PE solution for the sound field variability due to small variations of the sound speed have been derived [11], and it generalizes previous formulations of Hursky et al. [12] and Smith [13] for 3-D sound propagation and for better accuracy by employing the higher-order square root operator splitting algorithm, Eq. (1). Consider the following one-way parabolic wave equation,

$$\frac{\partial}{\partial x}u(x,y,z) = ik_{\text{ref}}\left\{-1+\sqrt{k_{\text{ref}}^{-2}\nabla_{\perp}^{2}+n^{2}(x,y,z)}\right\}u(x,y,z) \tag{2}$$

Here, the Cartesian coordinate system is selected to achieve a uniform resolution, and the parabolic wave equation can also be expressed in the same form using cylindrical coordinates. In Eq. (2), u is the demodulated sound pressure with the baseline phase removed according to the reference wavenumber k_{ref}, and n is the index of refraction with respect to the reference wavenumber. Now let $n^2 = \gamma_0 + \varepsilon\gamma_1$ and, as shown in [11], the higher-order tangent linear PE solution is

$$u(x+\Delta x) \cong e^{ik_{\text{ref}}\Delta x\mathcal{L}_0}\left[1+\frac{ik_{\text{ref}}}{2}\Delta x(1-\mathcal{L}_0)\varepsilon\gamma_1\right]u(x) \tag{3}$$

An example of 75 Hz sound propagation in an idealized slope environment is shown in Figure 1 to demostarte the accuracy of the higher order tangent linear solution.

Another example of the horizontal ducting of sound by a sound speed front over a slope is presented. The sound speed front is caused by a nonlinear internal wave of depression across the slope as shown in Figure 2(a). There are two layers in the water column, and the upper layer is 20-m thick with sound speed 1520 m/s, as opposed to 1480 m/s in the lower water layer. A 75Hz point source is placed between the apex and the internal wave (500m to the wave), and the source depth is 50 m. Figure 2(b) shows the background TL solution on the x-y plane at the source depth (50 m) in the absence of the internal wave, and one can see both the cut-off of the sound in the x direction and the interference pattern caused by the horizontal refraction of acoustic modes off the slope. Because the thermocline in the water column is depressed by the internal wave, a 3-D acoustic duct is formed. The higher-order

tangent linear solution shown in Figure 2(c) indeed captures the propagation physics. To examine the accuracy of the tangent linear solution, the higher-order split-step Fourier PE solution [5] is computed directly without using the perturbation formula. As seen in Figure 2(d), the higher-order tangent linear solution agrees with the direct solution very well. Note that, even though the acoustic ducting condition changes drastically due to the presence of the internal wave, the tangent linear solution can still accurately predict the effects of sound speed variations and track down the sound field variability.

2. 3-D sound propagation over a submarine canyon

The sound propagation effects caused by submarine canyons have also been studied in this year using the transmission loss (TL) data collected during the QPE experiment [8-9], where mobile acoustic sources were utilized to study sound propagation over North Mein-Hua Canyon. A 3-D PE model [4] is employed to explain the underlying physics. The acoustic data show a significant decrease in sound intensity as the source crossed over the canyons (see Figure 3), and the numerical model produces comparable results due to this shadowing effect. In addition, the model suggests that 3-D sound focusing due to the canyon seafloor can occur when the underwater sound propagates along the canyon axis.

A preliminary study has been performed to examine the effects of bathymetric and bottom property uncertainties. The first environmental uncertainty to be discussed is the bathymetry, which is the most important factor causing sound field complexity over a submarine canyon. Because bathymetric errors can transfer into TL errors through incorrect bottom interaction in a sound propagation model, it is important to have an accurate bathymetric map to ensure model accuracy. To examine the pre-QPE bathymetric database, the water depth data obtained from shipboard echo sounders during the 2009 QPE cruises were compared, and a specific comparison (Figures 3(d) and 3(e)) is made to show the difference in the modeled TL that result from using the two different bathymetric data sets. The propagation path runs across the canyon, and the two bathymetric datasets indeed produce different TL predictions. The most notable discrepancy is the interference pattern near the start of the track, but both models produce comparable shadow zones ranging from 4 to 7 km and extending to 200 m deep. This explains why the data and model comparison using the pre-QPE bathymetric database shows reasonable agreement. Also note the bottom reflection in the steep canyon (Figure 3(e)). Although the up-slope propagation terminates the shadow zone, the TL is large because the steep slope causes greater bottom loss.

The next environmental uncertainty to be considered is the bottom geoacoustic properties. Based on the understanding of strong currents in the canyon area, fine suspended sediments are not supposed to settle easily. So, a sandy bottom model is assumed for the numerical simulations with sound speed *cp* 1700 m/s, density 1.5 g/cm3 and attenuation coefficient 0.5 dB/λ. To present changes of the modeled TL due to different bottom properties, the same numerical computation is repeated with two other bottom sound speeds, 1600 m/s and 1800 m/s. The modeled TL distributions are shown in Figures 3(f) and 3(g) with comparisons to the measured mean TL data. The bottom model with *cp* = 1800 m/s does improve the TL comparison. This suggests that the real bottom is probably harder than what we expect, or that the bottom is more variable (i.e., consists of a number of different regimes) than was assumed. To make a stronger statement, we need to consider the bathymetric uncertainty that can also affect the predictability of bottom reflections. Such a joint uncertainty study will be performed later in the project.

3. Probability of dection of sound over a submarine canyon

The QPE canyon transmission data have also been used to obtain the probability of detection of sound over North Mien Hua Canyon (see Figure 4). The data processing method is briefed here. In each 1-

min transmission, there were six 2-s HFM sweeps and 48-s long CW tones. A portion of the acoustic data during the CW transmission (30 s) is processed with the short-time Fourier transform (STFT) to detect the 880 Hz CW signal. In each STFT step, a 2-s long signal is extracted and tapered with a Hamming window. It is then zero-padded to be ~13.4-s long to produce a high-resolution spectrum around the nominal frequency (880 Hz). The location of the greatest spectrum peak is recorded for computing the signal detection rate. To continue the process until the end of the 30-s data, the STFT window is moved in a 1-s interval, which results in totally 30 spectrum measurements. The ratio of the greatest peak of each spectrum locating within +/-0.5 Hz around the theoretical Doppler-shifted frequency is calculated, and it is the probability of detection of the 880Hz signal. The cross dots in Figure 4(c) are in fact the measured probability for every transmission within the processed window bounded by the lines shown in Figure 3(a). Note that the decreasing of the detection probability seen in Figure 3(c) is in fact caused by the shadowing effect of the sound propagating across the canyon explained in the preceding section.

4. Horizontal ducting of sound in a meandering internal wave duct

A numerical computation of horizontal ducting of sound in a meandering nonlinear internal wave field has been made. The wavefronts follow a sinusoidal function with a 200-m amplitude and a 20-km wave length. The internal wave curvature is 50.66 km at the most curved part, and it changes longitudinally along the duct. As sketched in Figure 5(a), the horizontal modes tend to be of whispering gallery type in the most curved part. On the other hand, the horizontal modes tend to be fully bouncing in the less curved portion because the concavity of the wavefront is not great enough to support whispering gallery ducting. Figures 5(b)–5(e) depict the horizontal ducting of vertical modes 1 and 2 for different source locations obtained from 3-D PE calculations. In this example where the source is placed in the curved part, when the source is close to the outer wave, more sound is trapped in the duct. This is because the whispering gallery modes in the curved part are excited. In this meandering wave case, we also notice that the horizontal modes have a longitudinal variation, because the internal wave curvature changes along the waveguide. In a more realistic situation, where the wave shape varies along the wavefront, the horizontal mode variation will be even more significant. The consequence is that the ducted sound will encounter horizontal mode coupling.

RESULTS

The major results of this project are summaried here, along with a publication list provided later. First, A higher-order tangent linear PE solution of 3D sound propagation has been derived, and it unifies other tangent linear PE solutions by employing a higher-order splitting algorithm for the square-root Helmholtz operator. Numerical examples of 3D sound propagation are presented to show the performance of the solution. The first example considers an idealized slope/wedge problem, and the higher-order tangent linear solution agrees very well with the reference solution obtained from the method of images. The second example is the horizontal ducting of sound by a sound speed front over a slope. It shows that the tangent linear solution can accurately predict the sound field variability even when the ducting condition changes drastically.

The QPE transmission data have been analyzed for sound propagation over the North Mien-Hua Canyon northeast of Taiwan. A pre-cruise numerical study showed a strong 3-D focusing effect caused by the concave canyon seafloor. Mobile acoustic sources were deployed to validate the model. However, the sources were pushed off of their planned tracks by the current, so we were not able to confirm the predicted focusing effect. Nonetheless, the field data still showed a shadowing effect, which is also an important factor in considering underwater sound propagation over a submarine canyon. A 3-D PE model was utilized to provide physical insights into the TL data. Acoustic shadow zones are identified in the numerical

model, and the resultant shadowing effect agrees with the measured data quite well. Model uncertainties due to incomplete measurements of the sound speed field, the seafloor topography and the sub-bottom structure are also noted, and it is left for future work to thoroughly evaluate the effect of each environmental uncertainty on the TL predictability. Bathymetric uncertainty could be the most important factor when considering sound propagation in a submarine canyon, and it will affect the TL predictions in conjunction with other environmental uncertainties. Incorporating ocean dynamic models to reduce water column uncertainty is suggested and currently being pursued by the authors and their collaborators.

Lastly, theoretical and numerical investigations of 3D sound propagation have been carried out to study effects due to meandering nonlinear internal waves. The study shows that the horizontal ducting of sound by curved internal waves has generally two types: whispering gallery modes and fully bouncing modes, and in order for the sound to be ducted by the meandering waves, the whispering gallery modes in the curved part need to be excited.

IMPACT/APPLICATIONS

The potential relevance of this work to the Navy is on increasing the capability of sonar systems in shallow water areas. The contributions of the effort on studying 3-D sound propagation effects will be on assessing the environment-induced acoustic impacts.

RELATED PROJECTS

Experimental data used during this year were collected from the ONR QPE project. Also, collabration with Drs. K.G. McMahon, J.F. Lynch, and W.L. Siegmann on studying horizontal ducting of sound in a meandering nonlinear internal wave field is through an ONR MURI project, Integrated Ocean Dynamics and Acoustics (IODA).

REFERENCES

[1] Y.-T. Lin and J.F. Lynch, "Analytical study of the horizontal ducting of sound by an oceanic front over a slope, " *J. Acoust. Soc. Am.*, vol. 131, pp. EL1-EL7 (2012).

[2] Y.-T Lin, T.F. Duda and J.F. Lynch, "Acoustic mode radiation from the termination of a truncated nonlinear internal gravity wave duct in a shallow ocean area", *J. Acoust. Soc. Am.*, vol. 126, pp. 1752-1765 (2009).

[3] Y.-T. Lin, K.G. McMahon, J.F. Lynch, and W.L. Siegmann, "Horizontal ducting of sound by curved nonlinear internal gravity waves in the continental shelf areas," *J. Acoust. Soc. Am*., vol. 133, pp. 37-49 (2013).

[4] Y.-T. Lin, T.F. Duda, and A.E. Newhall, "Three-dimensional sound propagation models using the parabolic-equation approximation and the split-step Fourier method," *J. Comp. Acoust.*, vol. 21, 1250018 (2013).

[5] Y.-T. Lin and T.F. Duda, "A higher-order split-step Fourier parabolic-equation sound propagation solution scheme," *J. Acoust. Soc. Am*, vol. 132, pp. EL61-EL67 (2012).

[6] Y.-T. Lin, J.M. Collis and T.F. Duda, "A three-dimensional parabolic equation model of sound propagation using higher-order operator splitting and Padé approximants," *J. Acoust. Soc. Am.*, vol. 132, pp. EL364-370 (2012).

[7] Y.-T. Lin, "A higher-order tangent linear parabolic-equation solution of three-dimensional sound propagation, " *J. Acoust. Soc. Am.*, vol. 134, pp. EL251-EL257 (2013).

[8] Gawarkiewicz, G. G., S. Jan, P. F. J. Lermusiaux, J. L. McClean, L. Centurioni, K. Taylor, B. 14 Cornuelle, T. F. Duda, J. Wang, Y. J. Yang, T. Sanford, R.-C. Lien, C. Lee, M.-A. Lee, W. 15 Leslie, P. J. Haley Jr., P. P. Niiler, G. Gopalakrishnan, P. Velez-Belchi, D.-K. Lee, and Y. Y. 16 Kim (2011). "Circulation and intrusions northeast of Taiwan: Chasing and predicting 17 uncertainty in the cold dome," Oceanography, vol. 24, pp. 110-121.

[9] A.E. Newhall, J.F. Lynch, G.G. Gawarkiewicz, T.F. Duda, N.M. McPhee, F.B. Bahr, C.D. Marquette, Y.-T. Lin, S. Jan, J. Wang, C.-F. Chen, L. Y.-S. Chiu, Y.-J. Yang, R.-C. Wei, C. Emerson, D. Morton, T. Abbot, P. Abbot, B. Calder, L.A. Mayer, and P.F.J. Lermusiaux, Acoustics and oceanographic observations collected during the QPE Experiment by Research Vessels OR1, OR2 and OR3 in the East China Sea in the Summer of 2009, Woods Hole Oceanographic Institution Tech. Report WHOI-2010-06, Woods Hole Oceanographic Institution, Woods Hole, MA, USA.

[10] Y.-T. Lin, T.F. Duda, C. Emerson, G.G. Gawarkiewicz, A.E. Newhall, B. Calder, J.F. Lynch, P. Abbot, Y.-J. Yang and S. Jan, "Experimental and numerical studies of sound propagation over a submarine canyon northeast of Taiwan," IEEE J. Ocean. Eng., submitted (2013).

[11] Y.-T. Lin, "A higher-order tangent linear parabolic-equation solution of three-dimensional sound propagation," J. Acoust. Soc. Am., vol. 134, pp. EL251-EL257 (2013).

[12] P. Hursky, M.B. Porter, B.D. Cornuelle, W.S. Hodgkiss, and W.A. Kuperman, “Adjoint modeling for acoustic inversion,” J. Acoust. Soc. Am. 115, 607–619 (2004).

[13] K.B. Smith, “Adjoint modeling with a split-step Fourier parabolic equation model (L),” J. Acoust. Soc. Am. 120, 1190–1191 (2006).

PUBLICATIONS

2013 **Y.-T. Lin**, "A higher-order tangent linear parabolic-equation solution of three-dimensional sound propagation," J. Acoust. Soc. Am., vol. 134, pp. EL251-EL257. [published, refereed]

2013 **Y.-T. Lin**, K.G. McMahon, J.F. Lynch, and W.L. Siegmann, "Horizontal ducting of sound by curved nonlinear internal gravity waves in the continental shelf areas," J. Acoust. Soc. Am., vol. 133, pp. 37-49. [published, refereed]

2013 **Y.-T. Lin**, T.F. Duda, C. Emerson, G.G. Gawarkiewicz, A.E. Newhall, B. Calder, J.F. Lynch, P. Abbot, Y.-J. Yang and S. Jan, "Experimental and numerical studies of sound propagation over a submarine canyon northeast of Taiwan," IEEE J. Ocean. Eng. [submitted]

2013 A.A. Shmelev, J.F. Lynch, **Y.-T. Lin** and H. Schmidt, "3D coupled mode analysis of internal-wave acoustic ducts," J. Acoust. Soc. Am. [submitted]

2013 L.Y.S. Chiu, A. Chang, **Y.-T. Lin**, and C.-S. Liu, "Estimating Geo-acoustic Properties of the Surficial Sediments in the Region of North Mein-Hua Canyon with a Chirp Sonar Profiler," IEEE J. Ocean. Eng. [submitted]

2013 C. Emerson, J.F. Lynch, P. Abbot, **Y.-T. Lin**, T.F. Duda, G.G. Gawarkiewicz and C.-F. Chen, "Acoustic Propagation Uncertainty and Probabilistic Prediction of Sonar System Performance in the Southern East China Sea Continental Shelf and Shelfbreak Environments," IEEE J. Ocean. Eng. [submitted]

2013 M.E.G.D. Colin, T.F. Duda, L.A. te Raa, T. van Zon, P.J. Haley Jr., P.F.J. Lermusiaux, W.G. Leslie, C. Mirabito, F.P.A. Lam, A.E. Newhall, **Y.-T. Lin**, and J.F. Lynch, "Time-evolving acoustic propagation modeling in a complex ocean environment," in Proceedings of Oceans '13 (Bergen) Conference, IEEE/MTS. [published, not refereed]

2013 T.F. Duda, **Y.-T. Lin** and B. D. Cornuelle, Scales of time and space variability of sound fields reflected obliquely from underwater slopes, Proc. Meet. Acoust., 19, 070025. [published, not refereed]

2013 J.F. Lynch, **Y.-T. Lin**, T. F. Duda and A. E. Newhall, "Characteristics of acoustic propagation and scattering in marine canyons", in Proceedings of the 1st International Underwater Acoustics Conference, Corfu, Greece. [published, not refereed]

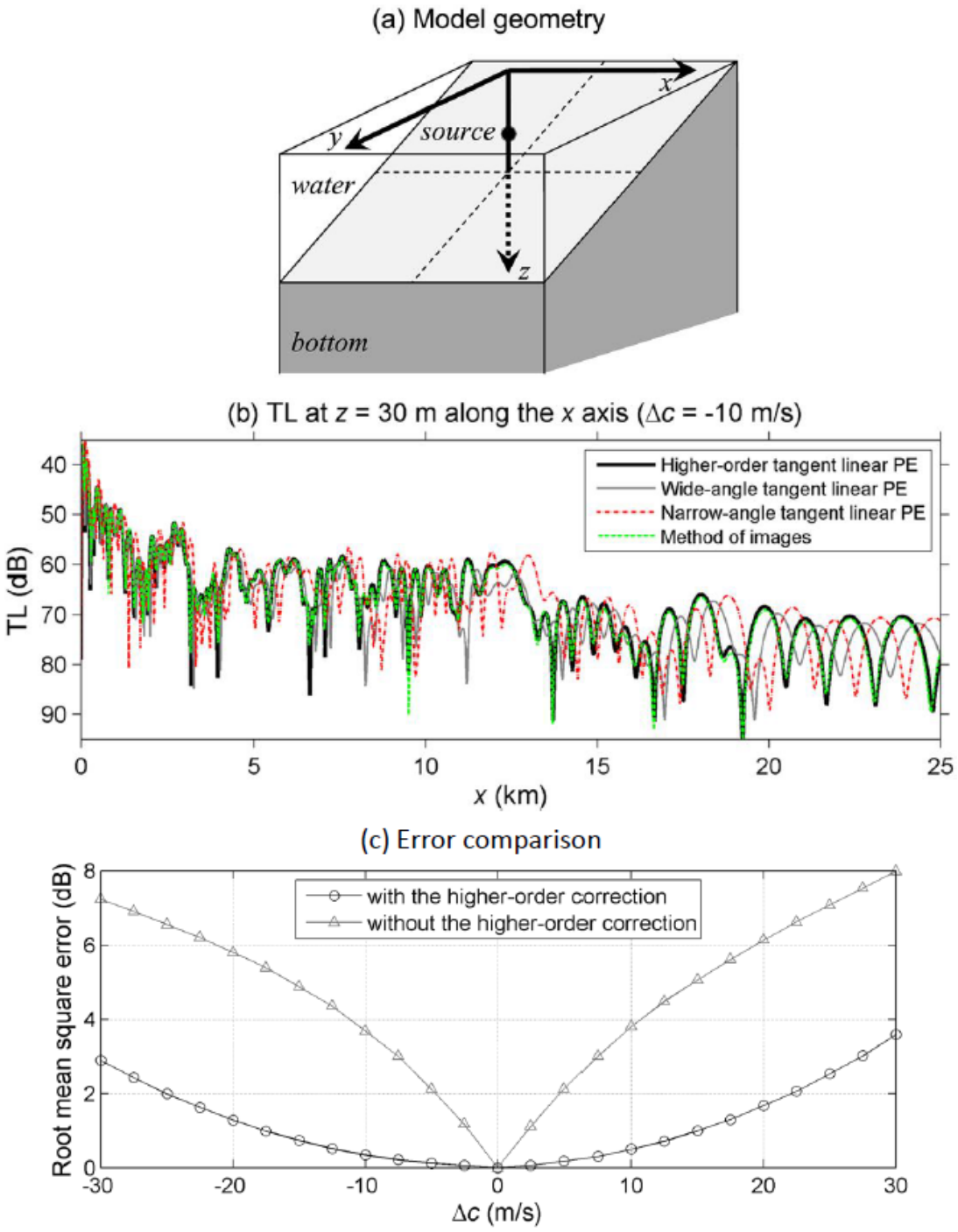

Figure 1. An example of 75 Hz sound propagation in an idealized slope environment the higher order tangent linear PE method.
[(a) Geometry of the slope model. (b) Comparison of Transmission loss (TL) solutions at z = 30m along the x axis. Among three different tangent linear PE solutions, the higher-order one has the best agreement with the reference solution obtained from the method of images.
(c) Error comparison of the higher-order tangent linear PE solution with and without the higher-order correction.]

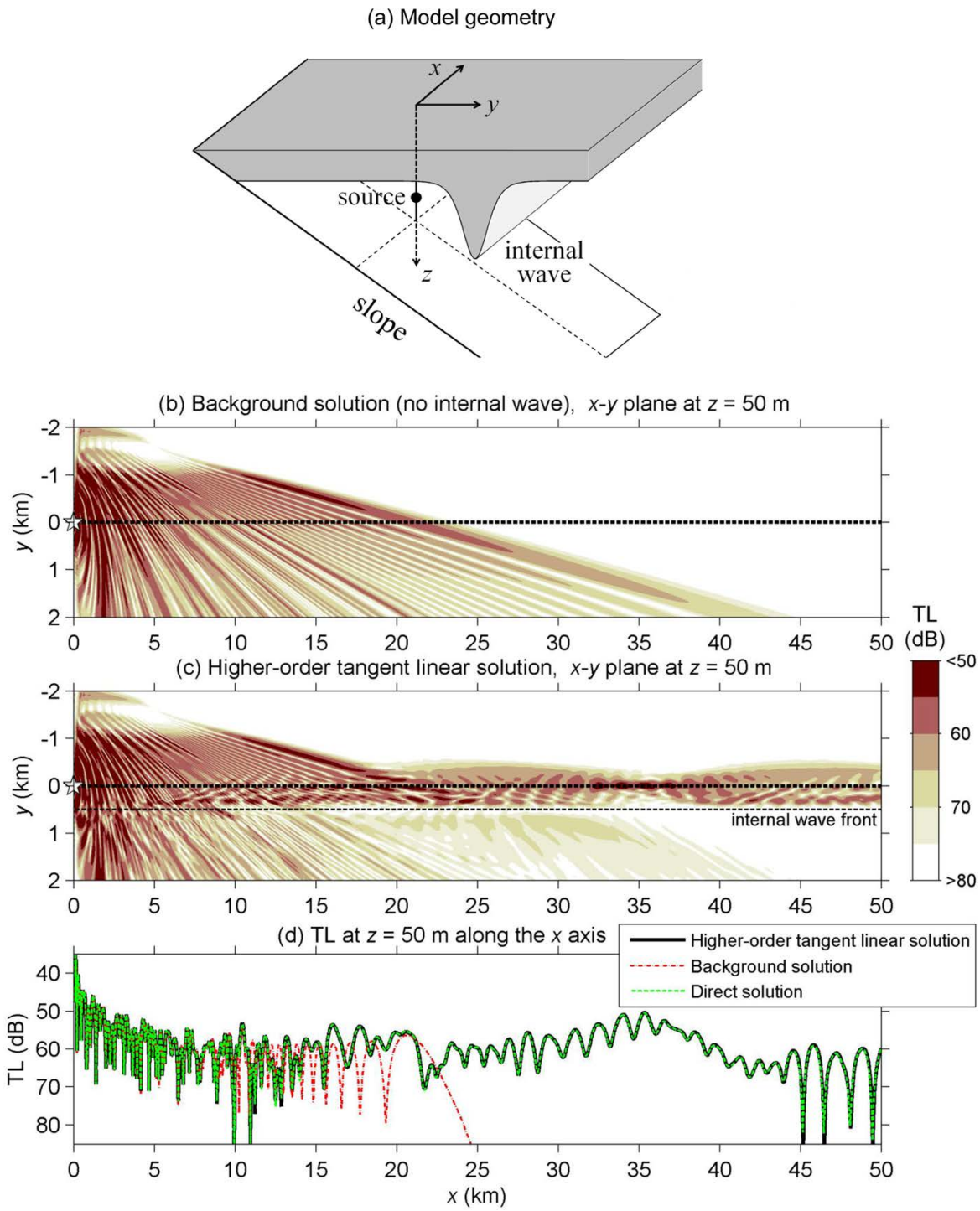

Figure 2. An example of 75 Hz sound propagation in the presence of a nonlinear internal wave over a slope.
[(a) Geometry of the slope plus internal wave model. (b) The background solution of the TL on the x-y plane at z = 50m in the absence of the internal wave. (c) The higher-order tangent linear PE solution of the TL on the x-y plane at z = 50m in the presence of the internal wave. (d) Comparison of different TL solutions.]

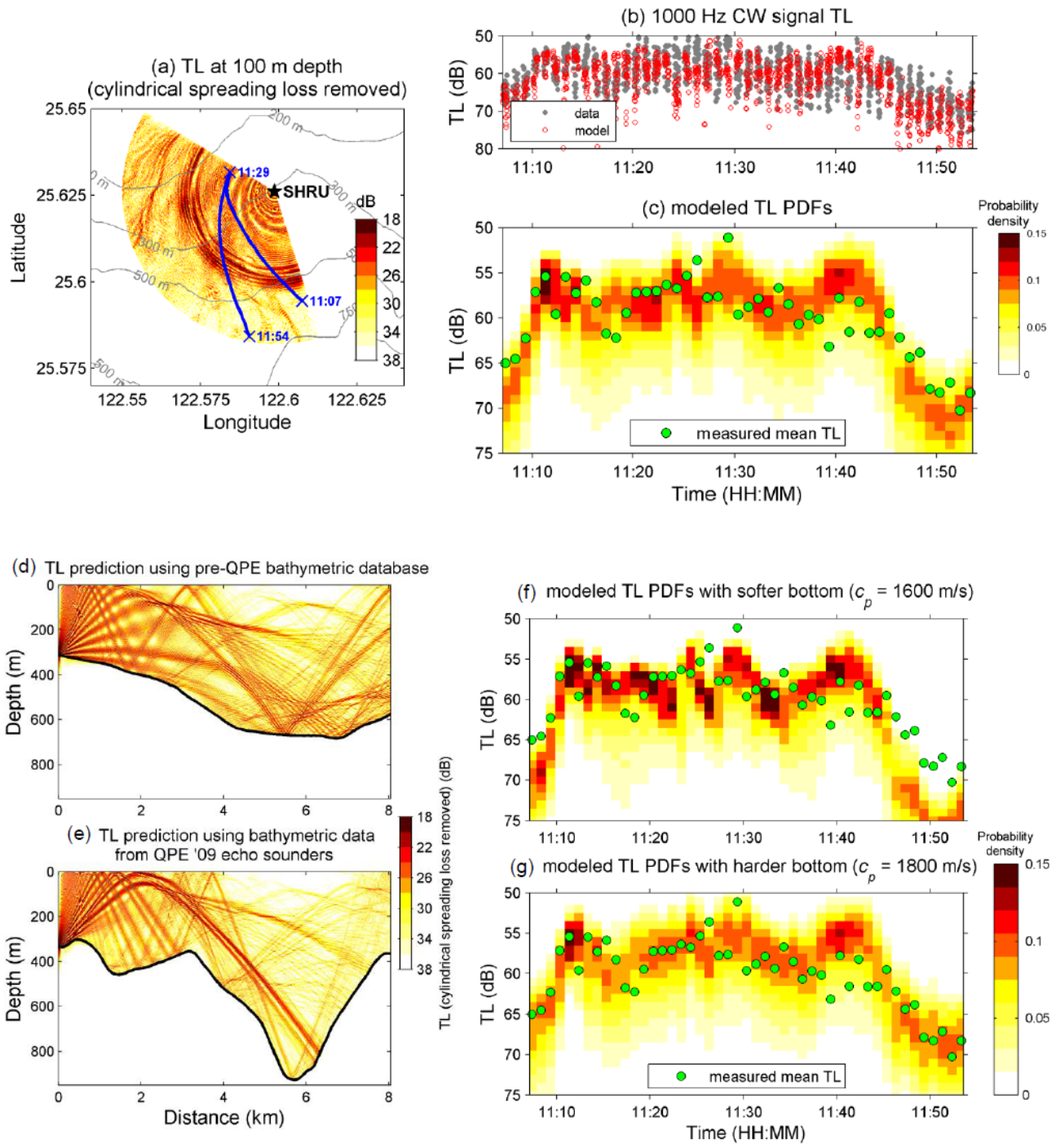

Figure 3. 3-D PE model TL and data comparison for the mobile source transmission in the QPE experiment over North Mein-Hua Canyon.
[The source track is denoted by the blue line in panel (a). The PE model TL and data are compared in a scatter plot (b) and a distribution (c). Panels (d) and (e) show the comparison of TL predictions resulted from two different bathymetric data. Panels (f) and (g) show the comparison of TL predictions resulted from two different bottom models. The bottom sound speed in the model shown in panel (c) is 1700 m/s.]

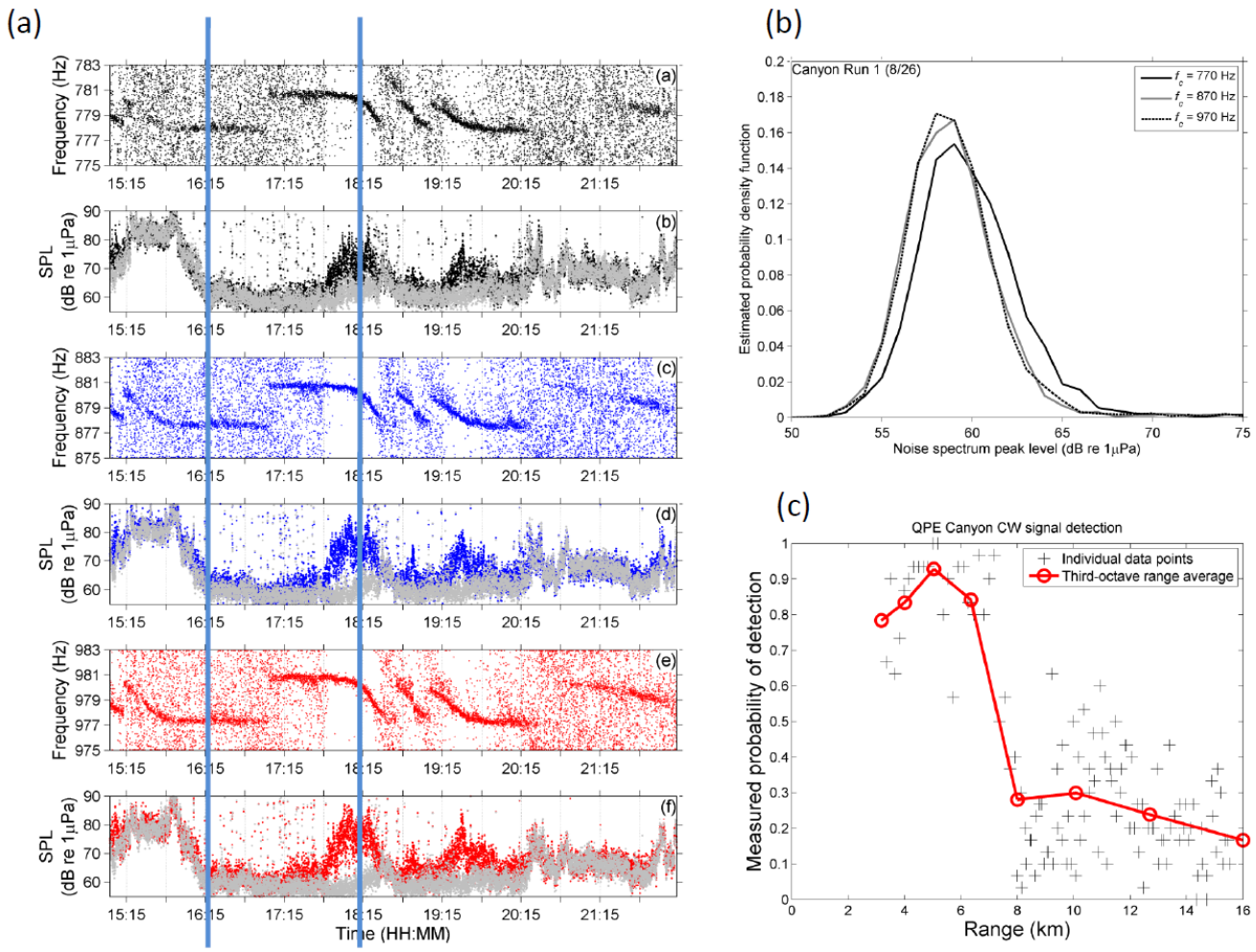

Figure 4. Probability of detection of sound over a submarine canyon. [(a) QPE canyon transmission data at three frequencies. The detected frequencies and sound pressure levels are shown. (b) The noise level distribution. (c) The cross dots are the measured probability for every transmission within the processed window between the lines in panel (a).]

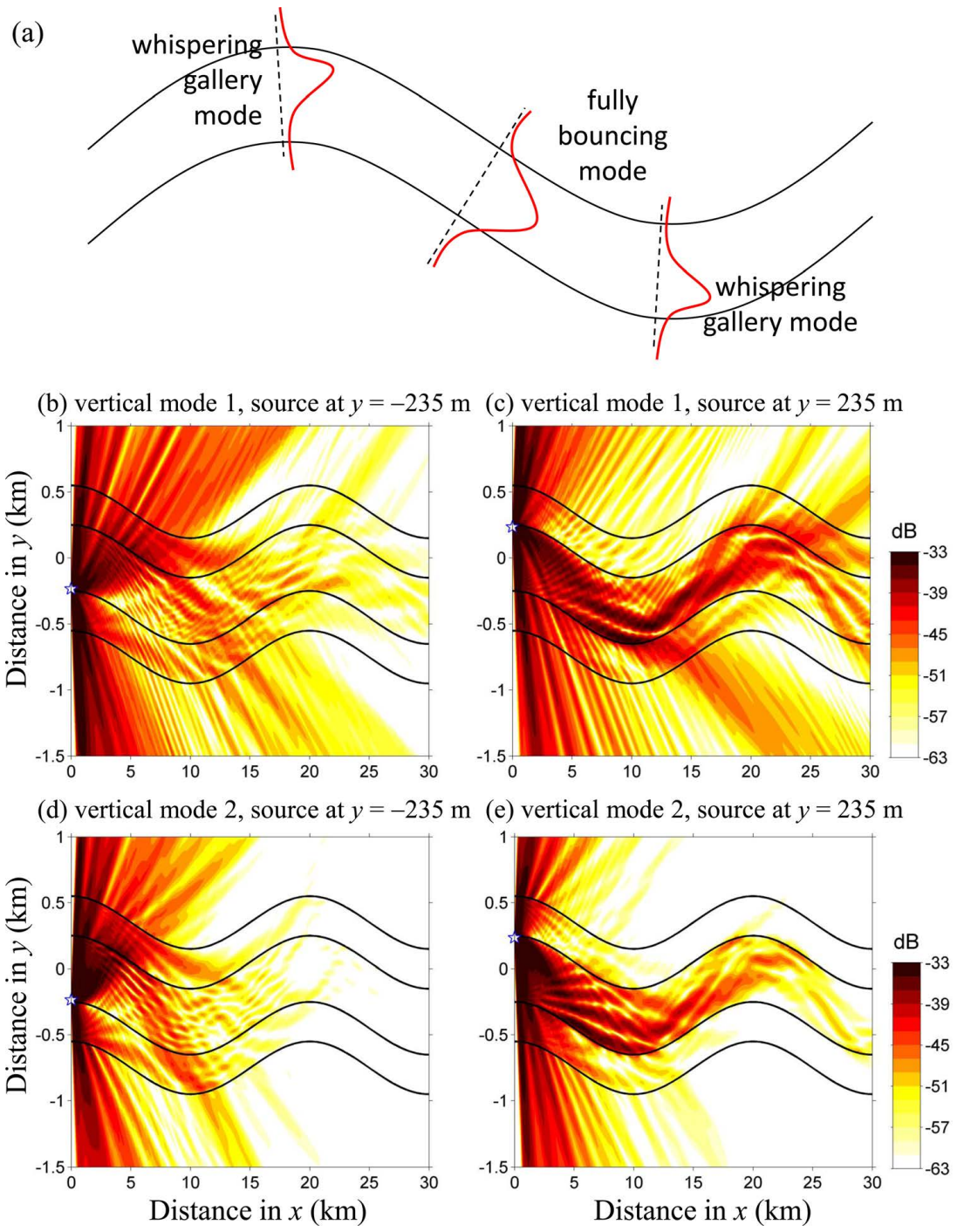

Figure 5. Horizontal ducting of sound in a meandering internal wave duct. [(a) A sketch showing different types of ducted modes in the duct. Full 3-D acoustic fields for a source in a curved portion and located (b) near the inner wave, and (c) near the outer wave. (d) Same as (b) except vertical mode 2 is plotted. (e) Same as (c) except vertical mode 2 is plotted.]